# Optimal Design and Analysis of a Hybrid Hydrogen Energy Storage System for an Island-based Renewable Energy Community

Zahir Dehouche * and Robert Garner *

Posted Date: 7 August 2023

doi: 10.20944/preprints202308.0471.v1

Keywords: Decentralised Energy Systems; Renewable Energy Community; Hydrogen Energy Storage System; Decarbonisation; Cost Optimisation

*Article*

# Optimal Design and Analysis of a Hybrid Hydrogen Energy Storage System for an Island-Based Renewable Energy Community

**Robert Garner [1] and Zahir Dehouche [1,*]**

[1] College of Engineering, Design and Physical Sciences, Brunel University London, Uxbridge, UB8 3PH, UK
* Correspondence: zahir.dehouche@brunel.ac.uk

**Abstract:** Installations of decentralised Renewable Energy Systems (RES) are becoming increasing popular as governments introduce ambitious energy policies to curb emissions and slow surging energy costs. This work presents a novel model for optimal sizing for decentralised renewable generation and hybrid storage system to create a Renewable Energy Community (REC), developed in Python. The model implements PV Solar and Wind Turbines combined with a hybrid battery and Regenerative Hydrogen Fuel Cell (RHFC). The electrical service demand is derived using real usage data from a rural island case study location. Cost remuneration is managed with an REC virtual trading layer, ensuring fair distribution among actors in accordance with the European RED(III) policy. A multi-objective Genetic Algorithm (GA) stochastically determines the system capacities suchthat the inherent trade-off relationship between project cost and decarbonisation can be observed. The optimal design results in an LCOE of 0.15€/kWh, reducing costs by over 50% compared with typical EU grid power, with a project IRR of 10.8%, simple return of 9.6%/year, and ROI of 9 years. Emissions output from grid only use is reduced by 72% to 69 gCO2e/kWh. Further research of lifetime economics and additional revenue streams in combination with this work could provide a useful tool for users to quickly design and prototype future decentralised REC systems.

**Keywords:** Decentralised Energy Systems; Renewable Energy Community; Hydrogen Energy Storage System; decarbonisation; Cost Optimisation

## 1. Introduction

The current state of the energy generation landscape is undergoing a significant change as concerns are raised over climate change, energy cost, and energy security. The aim as stipulated within the Paris Agreement [1] of keeping average surface temperature increase below 2°C by 2050 is extremely unlikely given global trends [2], and will be impossible without an ambitious sustainable energy development, financial investment and technological innovation [3]. Recent events on the global stage have caused nations in Europe and around the world to reconsider their energy security strategies [4,5]. The adoption of renewable energy at scale should include measures to improve the usage and effectiveness of non-renewable whilst providing cost reductions [6].

The introduction of Renewable Energy System (RES) including Photovoltaic (PV) solar panels and wind turbines have been the driving force removing global dependence on fossil fuels [7]. These types of RES are known as non-dispatchable as they are completely dependent on the weather conditions [8] and so cannot be precisely controlled. This becomes a problem for Transmission Service Operators (TSOs) as in that it creates a challenge for voltage and frequency balancing at a grid level [9]. The increasing volume of decentralized RES installed at the demand side is also a major problem for grid operators [10]. This induces bidirectional grid flows and puts additional strain on the network.

A solution to this problem is the use of Energy Storage Systems (ESS) to increase the share of the total RES production directly (self-consumption) [11] and local energy security [12]. Electro-chemical storage such as batteries have also been deployed in many cases for use as grid ESS [13–15], as they

 doi:10.20944/preprints202308.0471.v1



have the advantage of fast response to demand and can be installed in most global climates. Hydrogen storage can also be used for seasonal storage and only requires water as an input [16]. Hydrogen is also a flexible energy vector for many other uses such as heating and industrial processes [17]. A hybrid battery and hydrogen ESS has great potential to increase the share of renewables within the energy mix [18], thus decreasing the reliance on traditional power stations. The advent of widely available ESS has meant that it is now possible to emphasise self-consumption for energy at a local level to remove problems of grid stress and planning. In this way, a 'prosumer' (an end user that is able to both consume and produce energy [19]) or group of prosumers could install decentralised RES coupled with storage technology, if they are correctly incentivized by network operators, which classically only allow energy to be bought and sold via a utility company.

One of the solutions is the creation of decentralised Renewable Energy Communities (RECs). RECs in practice have many advantages and solve the most common issues associated with increased decentralised generation, while also promoting further installation and self-consumption of electricity. In a REC configuration, consumers and prosumers are no longer restricted to buying and selling energy from their utility company and can virtually 'share' the excess energy between actors within the energy community itself. This is mutually beneficial for both the network operator as they no longer have to manage unpredictable output from decentralised RES, and for the REC participants as they receive cost benefit and a reduction in carbon emissions.

The REC considered in this work is based on the policy recommendations recently implemented by a number of EU countries outlined in the Renewable Energy Directive (RED-II) (EU) 2018/2001 [20]. The directive defines a REC as *"a legal entity that is based on open and voluntary participation, it is autonomous and controlled by shareholders or members located in the proximity of renewable energy plants belonging to the community itself. The members may be physical persons, companies or local authorities..."*. While the directive has been transposed into several other national laws and decrees, including Austria [21], France [22], Germany [23] and the Netherlands [24], the REC modelled in this work mostly closely resembles the framework practiced in Italy as discussed by Trevisan et el. [25]. Although the study is in Spanish territory, it was chosen to follow the Italian implementation as there are more example cases available and, as of 2021, further improvements to the 2019 Spanish REC policy are currently in progress [26].

As laid out in decree-law 199/2021 [27], a group of self-consuming members within the REC must be located within the same Low-Voltage (LV) network downstream of the same LV/MV substation. Energy is shared of the existing physical network using a virtual network model. The difference between the energy consumed and energy produced by the REC is resolved over each one-hour period to determine the capacity available to be shared [28]. The model created in this work uses the principles of this decree to create the virtual REC.

A comprehensive energy model of the system is required to perform a techno-economic assessment to understand and assess the capacity of a REC to reduce cost and emissions for the participants, based on necessary local and regional policy. Optimal design of the model is also required such that the end users get the maximum economic and environment benefit from participating in the REC.

A number of studies including operational Renewable Energy Communities have assessment to understand and assess the capacity of a REC to reduce cost and emissions for the participants, based on necessary local and regional policy. Optimal design of the model is also required such that the end users get the maximum economic and environment benefit from participating in the REC.

A number of studies including operational Renewable Energy Communities have investigated the use of ESS within a REC to further improve the economic performance of centralised renewables. Trevisan et al. presented an optimised energy model considering PV solar and ESS to provide renewable power to a port REC, showing decrease in energy bills of 28% compared with the business-as-usual case [29]. Bartolini et al. investigated how to size a mixed RES to fully self-consume all generation at a community level, as well as meeting the heat energy needs, and showed that using hydrogen generation and storage is an economically viable alternative to battery systems [30]. Although less explored in literature, there have also been studies focused on the environmental and

 doi:10.20944/preprints202308.0471.v1



emissions reductions possible with such a community-based system. Wang et al. proposed a community-based Virtual Power Plant solution in Japan with PV and Battery ESS with the ability to reduce carbon emissions by 16.26% [31].

Several different modelling and optimisation software tools have also emerged to assist in model-based design and assessment. An in-depth review by Cuesta et al. presented popular renewable energy modelling tools, including ability to model different renewable assets and output different technical, economic, environmental, and social key performance indicators [32]. It's been noted that software such as HOMER, TRNSYS, and MATLAB/Simulink are most used due to their ease of use and available documentation. However, they can be restrictive for some REC cases due to their proprietary nature. Therefore, creating an open-source model in Python could provide the flexibility needed.

A number of optimisation procedures have been addressed and utilised in literature to determine the optimal design of hybrid RES and ESS. Most cases vary the design capacities to achieve one or more competing criteria such as economics, grid independence, and environmental impact. Niveditha and Rajan Singaravel consider a multi-objective design criteria for achieving Near Zero Energy Buildings (NZEB), using the functions of cost, Loss of Load Probability (LLP), and Total Energy Transfer (TET) to determine the best sizing arrangement for the PV-wind-battery storage system [33]. Zhang et al. presents a capacity configuration for both on-grid and off-grid mixed renewable system with hydrogen and batteries [34]. The NSGA-II algorithm is used to determine the trade-off relationship between system cost, renewable curtailment, and Loss of Load Probability (LLP), which can be considered analogous to grid independence for grid-connected configurations. Xu et al. considers the design of an off-grid PV-wind-hydrogen storage system using the multi-objective criteria of LCOE, LLP, and Power Abandonment Rate (PAR). The pareto optimal solution produces an LCOE of 0.226 $/kWh at acceptable LLP and PAR values [35]. It can be noted that studying the direct emissions associated with the grid independence would more accurately determine the positive environmental impact, which is of particular focus in this work. Results from literature also do not consider the implementation of such an optimisation procedure for RECs, and the impact of trading arrangements between members. Other algorithms including Multi-Objective Particle Swarm Optimisation (MOPSO) [36], and Multi-Objective Evolutionary Algorithm with Decision-Making (MOEA-DM) [37] have also been applied to ESS design, however NSGA-II remains the very popular and has proven robustness in energy flow optimisation problems [38].

## 2. Contribution

In this study, a techno-economic and carbon emissions assessment was conducted for a decentralised REC. The case study location was chosen as Formentera; a largely rural Balearic Island located in the Mediterranean Sea as illustrated in Figure 1. Emphasis is put on the isolated nature of the energy grid, which naturally increases the energy cost and embedded carbon of electricity usage, making it an ideal location for the study. A comparison of the base case scenario is used to compare the improvements made with the implementation of the REC. A novel energy systems model created in Python was used to determine the operating conditions of the combined energy generation and storage assets at a community level and shared between the community members. The study also uses real world load data collected from buildings on the island to create the hourly load profiles used in the modelling and simulation.

Preprints (www.preprints.org) | NOT PEER-REVIEWED | Posted: 7 August 2023 doi:10.20944/preprints202308.0471.v1



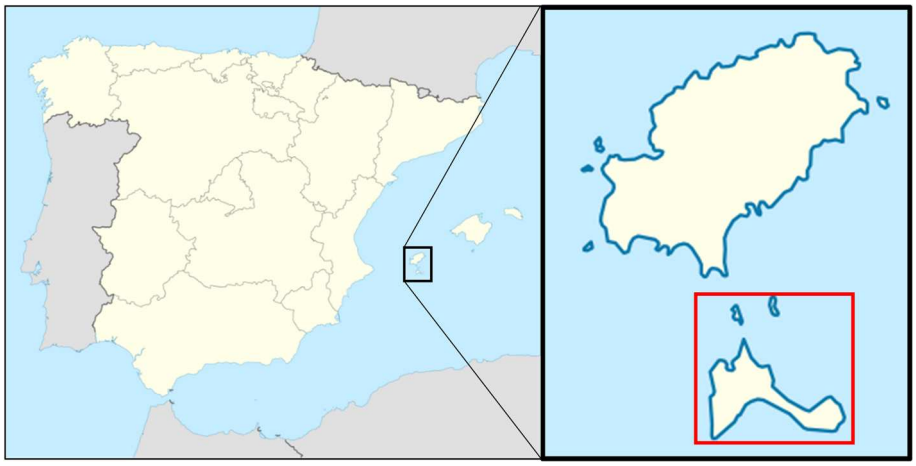

**Figure 1.** Formentera Island is located east of the Spanish mainland in the Mediterranean Sea.

The community has shared usage of PV solar and wind power to produce energy, and a hybrid battery and Regenerative Hydrogen Fuel Cell to store excess production. The combination of battery and hydrogen minimises the potential shortcomings of decentralised storage. A virtual trading scheme inspired by EU decree-law 199/2021 for REC implementation evaluates the portion of electricity shared among community members, without considering incentives or feed in tariffs. The methodology section explains the system modelling equations for each component, and the control logic used in the decision-making process to maximise the REC benefits. Technical, economic, and environmental parameters are added to the model to determine the system performance. This is followed by a multi-objective optimisation of the energy system component sizes to determine the best design topology based on cost and emissions reductions within the RECs boundary conditions.

Through the numerical simulation, the multi-objective results reveal the inherenttrade-off relationship between low-cost energy and the able to decarbonise supply, and that this approaches a critical limit at either extremes of the pareto front. This work also shows that across the pareto optimal sets, the hybridisation of energy storage provides better overall performance than a battery-only or hydrogen-only case. Additional constraints can be applied to the objective domain to assist in design decision-making.

The implementation of the model in Python allows for the creation of a scalable product, which following digitisation trends in model-based design could provide a vital tool for communities and policymakers to determine the best method for assisting communities to reach net-zero emissions.

## 3. Materials and Methods

The simulation model of the REC was developed in Python and assessed for its technical, economic, and environmental feasibility. For the purposes of simplification, the model is discretised into one hour time steps using kWh as the function unit for all energy flows within the system There is also the optimisation engine which house both single and multi-objective methodologies; the latter of which will be explored in this work. Firstly, The case study environment located on the island of Formentera, is defined, including building load and meteorological datasets as inputs for the simulation. The meteorological data at the chosen coordinate location was obtained from the National Aeronautics and Space Administration (NASA) Langley Research Center (LaRC) Prediction of Worldwide Energy Resource Project funded through the NASA Earth Science/Applied Science Program [39]. A combination of insight collected from the buildings about hourly, monthly, and yearly energy consumption where available was used to recreate the typical load profiles for each of the buildings within the Renewable Energy Community. A selection of 24 industrial, commercial, and residential load profiles produced by Farhad et al. (2020) were used to augment the profiles where a full set of data was incomplete [40]. This allowed for the definition of electrical load profiles for the seven members within the REC.

Preprints (www.preprints.org) | NOT PEER-REVIEWED | Posted: 7 August 2023 doi:10.20944/preprints202308.0471.v1



*3.1. Renewable Energy Community Implementation*

For the purposes of the design optimisation, it is assumed that the community members will have a shared investment in the generation and storage assets. A renewable generation system consisting of PV solar and wind power are used in combination to minimise moments of low energy production. These assets could either be installed in the low voltage energy grid within the same secondary substation of the REC, or spread out between the members, installing in open areas such as rooftops. The stationary ESS consisting of both a lithium-ion battery and a RHFC is installed at on the property of one of the community members, with capacity to accept but also release energy to the physical energy grid, such that it can be 'shared' virtually within the REC. A simple diagram of the system architecture is shown in Figure 2.

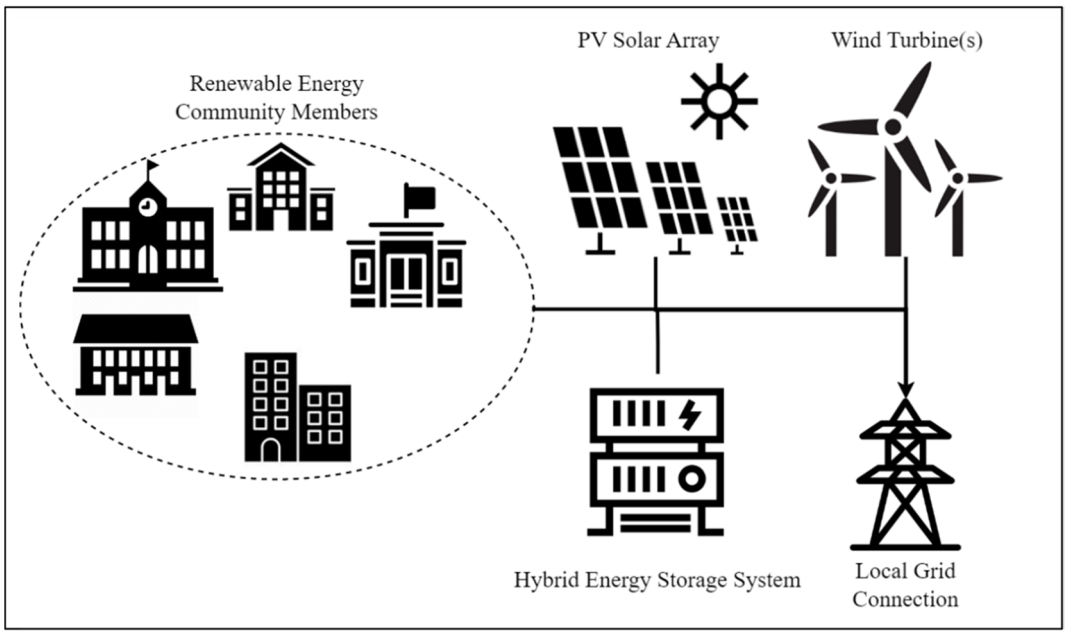


**Figure 2.** Renewable energy community system architecture.

The control strategy consists of load-following authority, but with additional considerations for the hybrid ESS. Since the battery performs better as a short-term storage, this discharges first to cover the load of the REC. Then, once the battery Depth-of-Discharge (DOD) limit is reached, the hydrogen system is used to cover the remaining demand. During the charging phase, this control scheme occurs in reverse. By evaluating the excess energy available between the total REC consumption and production over each one-hour increment in line with decree-law 162/19 for community implementation in Italy. The difference in this case is that the model does not consider incentives or tariffs to reduce financial strain and instead evaluates through a techno-economic assessment over a 20-year period whether the hybrid system is able to provide net-positive economic and environmental performance over the business-as-usual case.

*3.2. Renewable Energy Community Implementation*

The electrical load profiles form the foundation of the assessment of economic and environmental improvements to the REC. The community consists of seven member buildings; a community centre, a small school, a large school, local government offices, and three typical residential units. For the community centre, two schools, and offices, a sample daily load profiles as well as monthly average energy consumption was collected directly from the test site. For the residential units, a combination the annual heating, cooling, and appliances usage of 80.7 kWh/m2 was used to evaluation the typical characteristics of a residence in Spain [41], where the buildings were assumed to be 50 m2 in area. The monthly and yearly consumption was used to create a spline, over which the daily load profile was interpolated and repeated to create the one-year load profiles

Preprints (www.preprints.org) | NOT PEER-REVIEWED | Posted: 7 August 2023 doi:10.20944/preprints202308.0471.v1



for each building. Total yearly consumption for each member is included in Table 1, which the monthly and daily load profiles shown in Figure 3. The three mixed homes have been combined to represent a mixed family building and to improve visibility within the analysis.

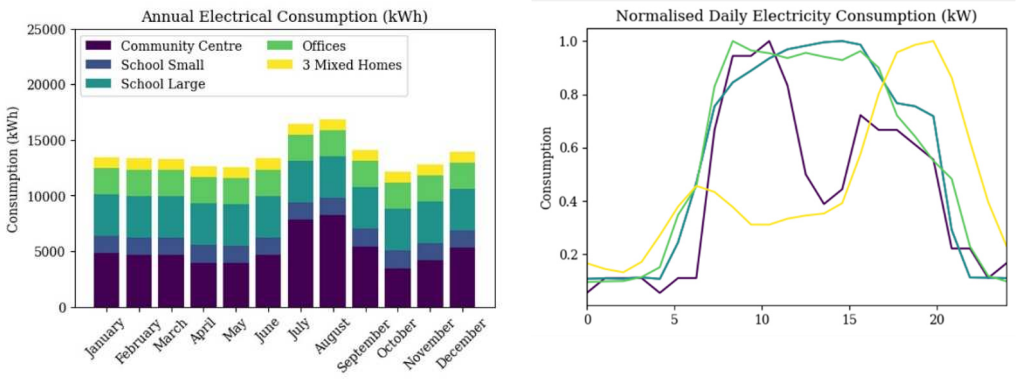


(**a**) Monthly electricity demand. (**b**) Normalised daily electricity demand.

**Figure 3.** Building electrical energy service demand model based on requirements of the Renewable Energy Community.

**Table 1.** Total annual electrical consumption for each member of the Renewable Energy Community.

| | **Annual Consumption** |
|---|---|
| Community centre | 66500 |
| Elementary school | 19200 |
| High school | 46200 |
| Government offices | 28900 |
| 3x Residential units | 12000 |

*3.3. Weather and Environment Data*

The weather data was collected for the year 2022 at the coordinate location of the chosen REC case study site. the model requires accurate measurements of ambient temperature, wind speed and global horizontal irradiance (GHI) solar conditions to evaluate the hour-by-hour power output of the renewable generation technologies. Figure 4 shows the hourly mean temperature and GHI for each month over one year. Higher GHI is observed in the summer period as expected in the northern hemisphere.

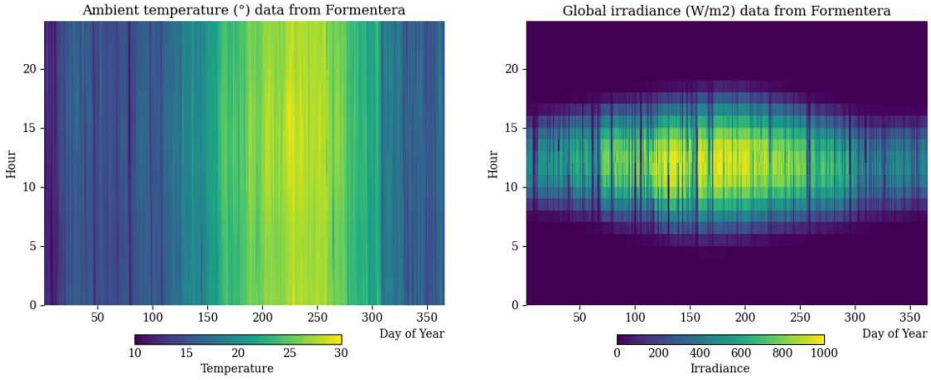


(**a**) Ambient temperature (°C). (**b**) Global horizontal irradiance ($W/m^2$)

**Figure 4.** Temperature and solar conditions over a one-year period at the island location. The weather conditions are assumed to remain constant year-on-year through the lifetime of the system.

Preprints (www.preprints.org) | NOT PEER-REVIEWED | Posted: 7 August 2023 doi:10.20944/preprints202308.0471.v1



*3.4. System Design and Characteristics*

3.4.1. PV Solar Array Model

The Mediterranean region's warm and dry climate promotes the use of PV solar systems to generate clean energy. For the purposes of the study, the solar array is assumed to be installed at 180° directly to the south, and at an optimal tilt angle of 38.7°. The power output of the solar panels $P_{PV}$ is modelled using the following governing equation [42]:

$$P_{PV} = C_{PV} d_f \left(\frac{G(t)_{module}}{G_{STC}}\right)\left[1 + \alpha_P\left(T_c - T_{c,STC}\right)\right] \quad (1)$$

Where $C_{PV}$ is the generation capacity (kW) of the solar installation under standard conditions, $d_f$ is the derate factor, $G(t)_{module}$ is the direct solar irradiance in $W/m^2$, $G_{STC}$ is the direct solar irradiance under standard test conditions (1000 $W/m^2$), $\alpha_P$ is the thermal power coefficient (%/°C), and $T_{c,STC}$ is the PV cell temperature under standard test conditions (25°C). $T_c$ is the PV cell temperature and is calculated by considering the measured Nominal Operating Cell Temperature (NOCT). NOCT is the cell measured temperature at a solar irradiance $G_{NOCT}$ of 800 $W/m^2$, an ambient temperature $T_{a,NOCT}$ of 20°C and a wind speed of 1 m/s [44]. This known thermal characteristic can then be used to adjust the cell temperature and find the corrected power output using the following equation [43]:

$$T_c = T(t)_a + \left(T_{c,NOCT} - T_{a,NOCT}\right)\left(\frac{G(t)_{module}}{G_{NOCT}}\right)\left(1 - \frac{\eta_{mp}}{\tau\alpha}\right) \quad (2)$$

Where $T(t)_a$ is the ambient temperature at timestep t and $\eta_{mp}$ is the cell efficiency. The constants $\tau\alpha$ can be assumed to be 0.9 for most cases. Since $\eta_{mp}$ is not known, the efficiency under standard conditions $\eta_{mp,STC}$ is substituted into the cell temperature equation above the result yields the following:

$$T_c = \frac{T(t)_a + \left(T_{c,NOCT} - T_{a,NOCT}\right)\left(\frac{G(t)_{module}}{G_{NOCT}}\right)\left[1 - \frac{\eta_{mp,STC}\left(1 - \alpha_P T_{c,STC}\right)}{\tau\alpha}\right]}{1 + \left(T_{c,NOCT} - T_{a,NOCT}\right)\left(\frac{G(t)_{module}}{G_{NOCT}}\right)\left[\frac{\alpha_P \eta_{mp,STC}}{\tau\alpha}\right]} \quad (3)$$

The GHI input data needs to be adjusted based on the local latitude $\varphi$ and module tilt $\beta$ to find the module irradiance $G(t, module)$ for the time of day and year. This is found with the following equations [44]:

$$G(t)_{module} = \frac{G(t)_{horizontal}\sin(\alpha + \beta)}{\sin\alpha} \quad (4)$$

$$\alpha = 90° - \phi + \delta \quad (5)$$

$$\delta = 23.45° \cdot \sin\left[\frac{360}{365}(284 + d)\right] \quad (6)$$

Where $G(t)_{module}$ is the module irradiance, $G(t)_{horizontal}$ is the GHI data, $\alpha$ is the elevation angle, and $\delta$ is the declination angle which deviates from the earth's tilt of 23.45° depending on the day of the year $d$.

3.4.2. Wind Turbine Model

A generic dynamic wind turbine model is used to calculate the expected power output in the selected location using the following [45]:

$$P(t) = \frac{1}{2} C_p \rho(t) A V^3(t) (\eta_m \cdot \eta_e) \quad (7)$$

Where $C_p$ is the power coefficient, $\rho(t)$ is the air density at the hub height, $A$ is the selected swept area in $m^2$, V(t) is the wind speed in m/s at the time step t, $\eta_m$ and $\eta_e$ are the mechanical and electrical

Preprints (www.preprints.org) | NOT PEER-REVIEWED | Posted: 7 August 2023 doi:10.20944/preprints202308.0471.v1



efficiencies. The wind speed is usually measured at different height compared to the hub height, $Z_{hub}$. Therefore, the model uses the logarithmic law to derive the hourly wind speed at the hub height as follows [45]:

$$V_{hub} = V_{anem}\left(\frac{\ln\left({}^{Z_{hub}}/_{Z_0}\right)}{\ln\left({}^{Z_{anem}}/_{Z_0}\right)}\right) \tag{8}$$

Where $Z_0$ is the surface roughness length (m), $Z_{anem}$ is the anemometer height (m), $V_{hub}$ is the wind speed at the required hub height (m/s), and the $V_{anem}$ is the measured wind speed at the anemometer height (10m for the dataset used). For simplicity, $C_p$ is evaluated by way of a 2D-look up table based on the four classes of wind turbines described in IEC 61400 standard [46]. The average wind speed and distribution is evaluated and the most appropriate characteristic is chosen from the four available classes ranked from low to high wind speeds [47]. The normalised power range for each class of "Offshore", "IEC-1", "IEC-2", and "IEC-3" are show in Figure 5a. The energy output over the course of one year can also be determined analytically by assessing the wind speed distribution. The Rayleigh distribution, shown in Figure 5b, has been overlaid to show that the wind speed distribution data follows this statistical law, which indicates that the normalised power curves will operate effectively for the model.

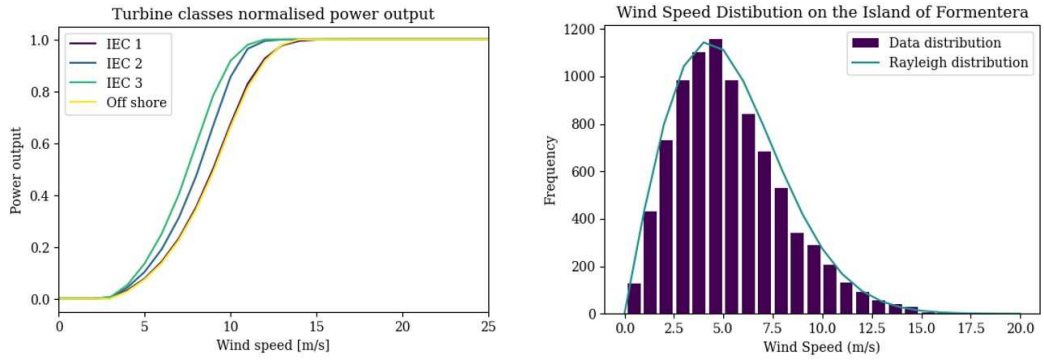


(**a**) Turbine normalised power output curve. (**b**) Wind speed distribution at Formentera.

**Figure 5.** Wind model input assumptions are primarily a combination of standardised wind turbine power coefficients and the load wind speed data measured at 10m above sea level.

3.4.3. Lithium Ion Battery Model

The battery model utilises a simplified version of the Shepard battery model [48], replacing internal and other resistive losses with a total charge $\eta_{charge}$ discharge $\eta_{discharge}$ efficiency for the hourly discharge case. The simplification allows for less information to known about the chemistry and dynamics of the specific battery to perform calculations for current capacity, and State of Charge (SOC). The battery system contains two parts: a charge model and a discharge model. The models take the power requirement from the battery and outputs the resulting SOC for the end of the timestep. These parts are defined as follows:

$$\begin{cases} SOC(t+1)_{batt} = \dfrac{Q(t)_{batt} + \int P(t)_{batt}\eta_{charge}\,dt}{Q(t_0)_{batt}} \cdot 100, & \text{charging} \\ SOC(t+1)_{batt} = \dfrac{Q(t)_{batt} - \int P(t)_{batt}\eta_{discharge}\,dt}{Q(t_0)_{batt}} \cdot 100, & \text{discharging} \end{cases} \tag{9}$$

Where $SOC_{t+1,batt}$ is the next timestep battery SOC, $Q_{t,batt}$ is the battery state of charge at timestep t, $Q_{t0,batt}$ is the initial SOC, $P_{t,charge}$ is the average charge power draw, and $P_{t,discharge}$ is the discharge power draw. These outputs are subject to the minimum and maximum SOC limits $SOC_{min}$ and $SOC_{max}$. The model includes degradation in the battery capacity linearly as a function of charge cycles, as shown below:

Preprints (www.preprints.org) | NOT PEER-REVIEWED | Posted: 7 August 2023 doi:10.20944/preprints202308.0471.v1



$$Q(l,t)_{batt} = Q(t_0)_{batt} - \alpha l \tag{10}$$

Where $Q(l, t)_{batt}$ is the dynamic capacity in kWh as a function of cycles the cycles $l$, and $\alpha$ is the ageing factor (kWh/cycle).

3.4.4. Regenerative Hydrogen Fuel Cell

The RHFC model provides an alternative energy storage facility to the electrochemical battery. The model consists of a PEM fuel cell and PEM electrolyser capable of consuming and producing hydrogen, respectively. The system also considers a hydrogen storage module with its own rated capacity and efficiency. The overall equations are like that of the simplified battery model in that the electrolyser and fuel cell analogously represent the charge and discharge elements. The system can therefore be shown as the following:

$$\begin{cases} Q(t+1)_{H2} = Q(t)_{H2} - \int P(t)_{fc}\eta_{fc}\,dt & \text{Fuel Cell} \\ Q(t+1)_{H2} = Q(t)_{H2} - \int P(t)_{el}\eta_{el}\,dt & \text{Electrolyser} \end{cases} \tag{11}$$

Where $Q(t+1)_{H2}$ is the next timestep hydrogen energy stored (kWh), $Q(t)_{H2}$ current timestep hydrogen energy stored (kWh) $P(t)_{fc}$ is the average fuel cell power production [kW] in the current one-hour timestep $t$, $P(t)_{el}$ is the average electrolyser power consumption [kW]. $\eta_{fc}$ and $\eta_{el}$ are the average lifetime fuel cell and electrolyser efficiencies [%], respectively. Like the battery, these energy values are also subject to $Q_{H2,min}$ and $Q_{H2,max}$ limits.

3.4.5. Model Input Assumptions

Table 2 contains the necessary input assumptions for the energy models, including efficiencies and other system dynamics that determine the output power generated or stored. The PV panel characteristics are based on the Sunpower Maxeon panel series, while the wind turbine is an approximation of common small scale turbine systems on the market. The roughness length assumption of 0.05 is defined as rural, farmland area with low crops and without many trees [49]. The hydrogen system efficiency values are based on industry knowledge gathered from leading European fuel cell and electrolyser manufacturers.

**Table 2.** Hybrid renewable energy system design input assumptions across the different included technologies.

| **PV solar** | |
|---|---|
| Panel Power (W) | 400 |
| Panel Area (m2) | 2 |
| Thermal Coefficient (%/°C) | -0.3 |
| NOCT (°C) | 42 |
| Lifetime (years) | 20 |
| **Wind turbine** | |
| Hub Height (m) | 20 |
| Roughness Height (m) | 0.05 |
| Lifetime (years) | 20 |
| **Lithium battery** | |
| Total Efficiency (%) | 95 |

Preprints (www.preprints.org) | NOT PEER-REVIEWED | Posted: 7 August 2023 doi:10.20944/preprints202308.0471.v1



| | |
|---|---|
| Maximum Cycles | 8000 |
| Maximum Age (years) | 10 |
| **Regnerative hydrogen fuel cell** | |
| Fuel Cell Efficiency (%) | 46 |
| Electrolyser Efficiency (%) | 68 |
| Lifetime (years) | 20 |

### *3.5. Energy Management Strategy*

The Energy Management Strategy for the hybrid storage system is shown in Figure 6. When generation supply is available in excess of demand, the battery charges first, followed by the larger capacity hydrogen storage via the electrolyser. When the demand outgrows the supply, the battery discharges first, followed by the activation of the fuel cell. In practical terms, the battery is actually being charged by the fuel cell while active, as the fuel cell cannot module its output without incurring performance losses. The charge and discharge states are is shown in Figure 6.

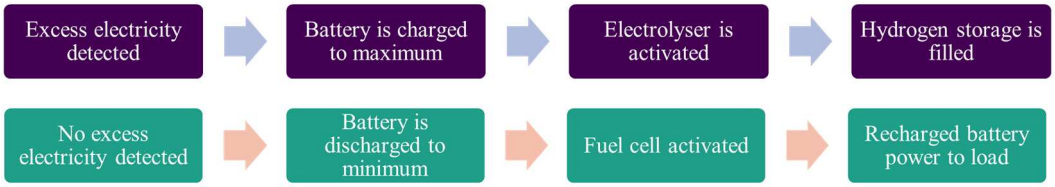


**Figure 6.** Energy management strategy of the hybrid storage system.

Virtual trading is used to fairly satisfy the community members based on the shared energy available. The excess energy available is shared equally, satisfying each load in ascending order of magnitude. This means that it is more likely that a member electricity demand will be fully satisfied if smaller. It should be noted that this algorithm can be modified to suit any location specific REC policy.

### *3.6. Economic and Environmental Indicators*

A selection of three different system configurations; best economic outcome, best environmental outcome, and a midpoint configuration between the two would be assessed in the model. It is important from a financial perspective to understanding the investment requirements and expected returns for prospective REC members. Net Present Value (NPV) is commonly employed to determine economic feasibility, as well as Internal Rate of Return (IRR), simple return [%], payback period [years], and Levelised Cost of Electricity (LCOE) for energy specific cases. Generally, if the NPV is positive compared to the base scenario the investment is worthwhile [50].

$$NPV = \sum_{n=1}^{N} \frac{C_{O\&M,n} + C_{f,n}}{(1+R)^n} - C_0 \quad (12)$$

Where $C_{O\&M,t}$ is the operation and maintenance cashflow for year $t$, $C_{f,t}$ is the fuel input cashflow, $R$ is the discount rate, and $C_0$ is the initial capital investment. It is assumed that any grid consumption is included in $C_{f,t}$ in units of €/year. The capital requirement and operating cashflows are summed for each generation and storage asset to solve for the system NPV. The IRR evaluates the rate of return if the NPV is set to zero, at which the project breaks even.

$$0 = \sum_{n=1}^{N} \frac{C_n}{(1+IRR)^n} \quad (13)$$

Preprints (www.preprints.org) | NOT PEER-REVIEWED | Posted: 7 August 2023 doi:10.20944/preprints202308.0471.v1



Calculating the LCOE is beneficial when the economic feasibility of different technologies. The LCOE was evaluated against the grid cost to assess the cost savings per unit of electricity could be expected by the community members. LCOE is defined as the total cost lifetime cost of the asset divided by the total electricity delivered to the consumer [51].

$$LCOE\left(\frac{€}{kWh}\right) = \frac{\sum_{n=1}^{N} C_{0,n} + C_{O\&M,n} + C_{f,n}}{\sum_{n=1}^{N} E_n} \quad (14)$$

Where $C_{0,n}$ is the capital cost of the asset, and $E_n$ is the lifetime energy delivered. A range of different assessments exist for the economics of renewable assets, as it is highly dependent on the capital requirement, location, delivery and installation cost, and available labour among other factors. The resulting CAPEX, OPEX, and lifetime parameters are shown in Table 2. The costs include the Balance of Plant (BOP), such as DC-AC inverters and IoT control equipment. The project has an assumed discount rate R of 5% and an estimated inflation rate of 2% per year, as well as a year one electricity grid unit cost of 0.30€/kWh for each building.

The environmental impact is estimated through the Global Warming Potential (GWP) of the assets, which when summed together and divided by the total energy delivered over the system lifetime derives the emissions intensity, measured in gCO2e/kWh. The values are then compared with the grid emissions intensity for the island, for which the total decarbonisation potential is evaluated. The grid emissions were found using generation data gathered from the national TSO (Red Electrica de Espana) for the year 2021 and found to have an average of 325 $gCO_2e$/kWh.

$$EI_{total} = \frac{\sum_{j=1}^{m}(EI_j \cdot E_j)}{\sum_{j=1}^{m}(E_j)} \quad (15)$$

$EI_j$ is the emissions intensity and $E_j$ is the energy output for $m$ number of generators and energy storage systems. This calculation is performed for each timestep of the simulation to find the dynamic emissions value depending on the instantaneous energy mix of the REC. The emissions intensity found within literature can vary due to the range of manufacturing techniques and factors considered when performing the Life Cycle Assessment (LCA). For this reason, some values such as the used for the hydrogen system are taken as an educated estimation of the emissions impact based on a variety of sources. The GWP embedded during manufacturing and installation for the assets are shown in Table 3.

**Table 3.** Hybrid renewable energy system economic and climate impact assumptions for the different modelled technologies.

| Technology | CAPEX | OPEX | Lifetime | Embedded Emissions |
|---|---|---|---|---|
| PV Solar Array [51–53] | 2500 €/kW | 30 EUR/kW/year | 20 years | 1826 kgCO2e/kW |
| Wind Turbine [54,55] | 2850 €/kW | 32 EUR/kW/year | 20 years | 520 kgCO2e/kW |
| Lithium-Ion LFP [56,57] | 389 €/kWh | 5 EUR/kWh/year | 10 years or 8000 cycles | 254 kgCO2e/kWh |
| PEM Fuel Cell [56,58] | 1200 €/kW | 13 EUR/kW/year | 20 years | 73.3 kgCO2e/kWh |
| AEM Electrolyser [56,59,60] | 1500 €/kW | 14 EUR/kW/year | 20 years or 35000 hours | 239 kgCO2e/kWh |

Preprints (www.preprints.org) | NOT PEER-REVIEWED | Posted: 7 August 2023 doi:10.20944/preprints202308.0471.v1



| | | | | |
|---|---|---|---|---|
| Hydrogen Storage Vessel [61–63] | 30 €/kWh | - | 20+ years | 5.1 kgCO2e/kWh |

 doi:10.20944/preprints202308.0471.v1



*3.7. Multi-objective optimisation procedure*

Designing and configuring the optimal system sizing for a hybrid decentralized energy system is a complex process. There are a number of non-linear phenomena being simulated, as well as many potential design objectives and constraints. The chosen objective functions considering both cost and carbon reduction are the NPV and the equivalent GWP. The objective functions rely on varying the capacities of the PV solar, wind, battery, and RHFC installations at the site.

The NSGA-II uses a heuristic evolutionary learning algorithm with a population of potential design solutions within the defined constraints. It then ranks the population based on a non-dominated sorting, producing a pareto front of optimal solutions by minimizing both objective functions [33]. Each individual in the population is determined based on the simulation of the model of a one-year period and evaluating the two objectives. The best performing individuals are passed to the next generation, whereas a combination of mutations and created offspring (crossover) determines the remaining individuals. NSGA-II provides several advantages including the use of elitism and reduced computational complexity [64]. The solving process for NSGA-II implementation is shown in Figure 7. The algorithm also requires inputs, including the population size, number of offspring, stopping conditions and variable constraints, as shown in Table 3. The lower limit for all system assets is set to zero, while the upper limit as set to 200 kW in line with the adopted REC regulation for this study. The *pymoo* module created and maintained by Blank et al. [65] was used to implement the NSGA-II algorithm in Python.

**Table 4.** Total annual electrical consumption for each member of the Renewable Energy Community.

| Parameter | Value |
|---|---|
| Population Size | 72 |
| No. of Offspring | 24 |
| Max No. of Generations | 400 |
| Lower Bounds (all assets) | 0 kW/kWh |
| Upper Bounds (all assets) | 200 kW/kWh |

Preprints (www.preprints.org) | NOT PEER-REVIEWED | Posted: 7 August 2023 doi:10.20944/preprints202308.0471.v1



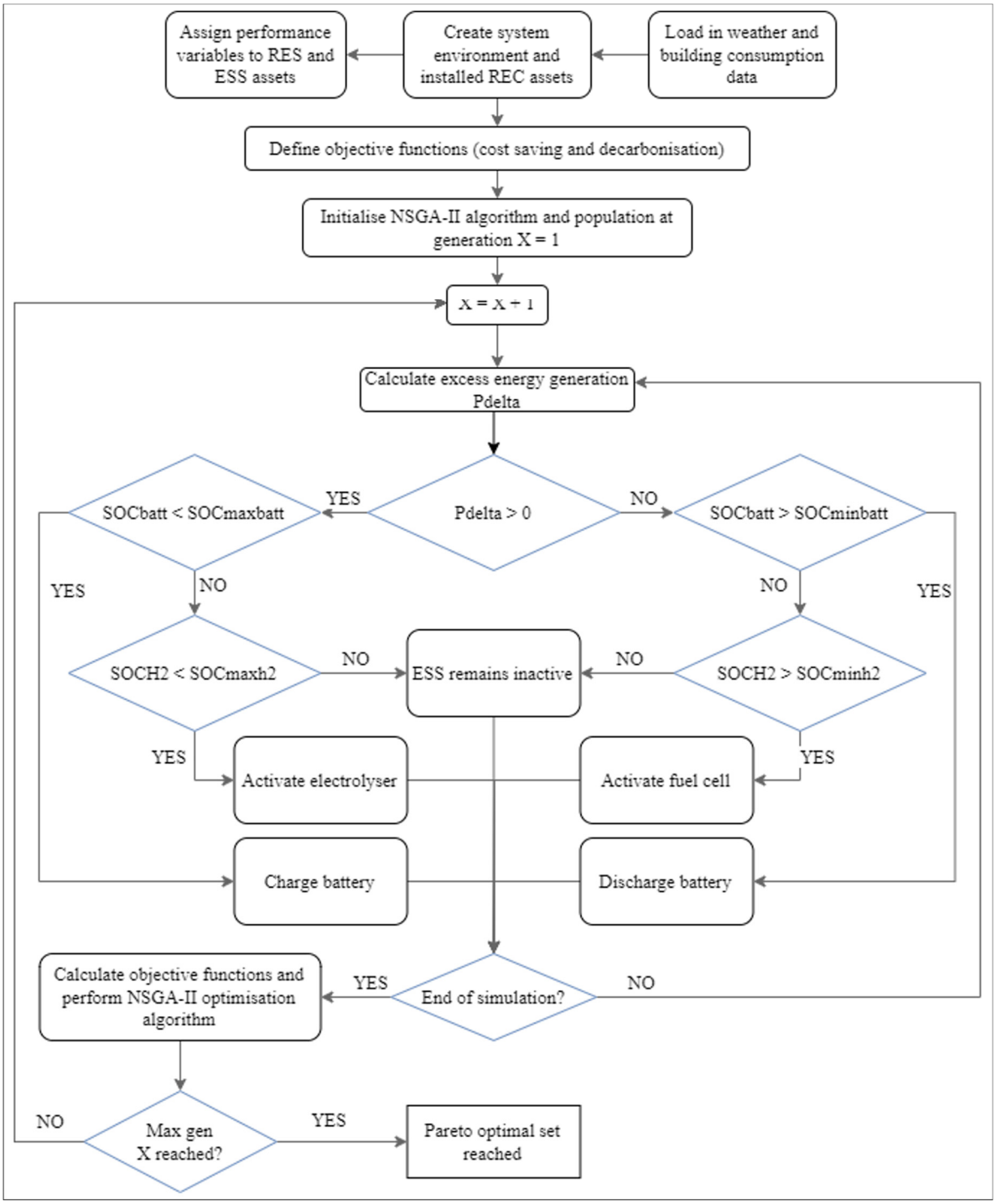


**Figure 7.** Hybrid energy system model approach with multi-objective optimisation algorithm NSGAII solving process.

The input parameters were set into the simulation model with the selected objective functions and run within the NSGA-II algorithm. The optimisation ran to the maximum allowed generations before terminating. Due to the bound nature of the problem, the component capacity variables start as a random distribution, from which the non-dominated solutions on the pareto front are selected. Well-performing individuals are moved forward to the next generation, as well as a selection of offspring and individuals that have experienced random mutation. As the generations progress, the population steadily converges on a large set of non-dominated solutions that align with the pareto front between best system economics and decarbonisation performance, denoted by the objective functions of cost savings and emissions intensity. The graph in Figure 8 shows the convergence of

Preprints (www.preprints.org) | NOT PEER-REVIEWED | Posted: 7 August 2023 doi:10.20944/preprints202308.0471.v1



the objective function products during the progression through the first 200 generations of the hybrid system optimisation, which will converge towards a single value.

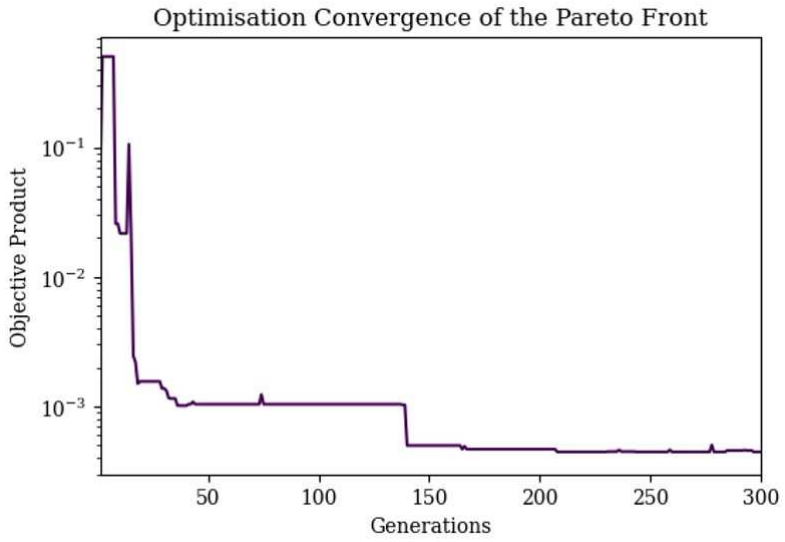


**Figure 8.** Convergence of the optimisation pareto front as shown by an aggregated scalar objective function minimising towards a single value.

## 4. Results and Discussion

### *4.1. Optimisation results of the hybrid energy generation and storage Renewable Energy Community*

The primary case studied was the hybrid architecture consisting of both a lithium battery and a RHFC. Within the resulting pareto front in Figure 9a, each point on the graph represents a different combination of design capacities ranging from the configuration able to achieve the highest economic returns to the system able to deliver the lowest net carbon output. The lifetime cost savings potential ranges from approximately 130k€to 186k€, while the emission intensity ranges from 82 to 140 gCO2e/kWh. It is interesting to note that the savings do not start at zero, implying that below 130k€returns the configuration is able to increase in economic performance as well as decarbonisation before reaching an inflection point. At this point, it is clear that the net savings are able to continue increasing, while the net emissions reaches its minimum and begins to climb again. At the other end of the front, the gradient begins to increase as both the returns increase but also the emissions intensity. This continues up to the point where the system can no longer provide additional savings without an exponential increase in embedded emissions and therefore environmental impact..

The resulting pareto front presents several crucial outcomes and challenges for providing a low cost and net-zero energy system. Firstly, an inherent trade-off relationship is observed between the ability to decarbonise and ensure net profitability. Secondly, the REC architecture, within the context and constraints of the study, can reduce carbon emissions by over 75% compared to local grid usage. However, this is a hard limit due to the capacity factors of the components and the embedded carbon within the system during manufacturing. additionally, trying to decrease the carbon emissions further only incurs a financial penalty, which would be hard to incentivise to the REC members.

Preprints (www.preprints.org) | NOT PEER-REVIEWED | Posted: 7 August 2023 doi:10.20944/preprints202308.0471.v1



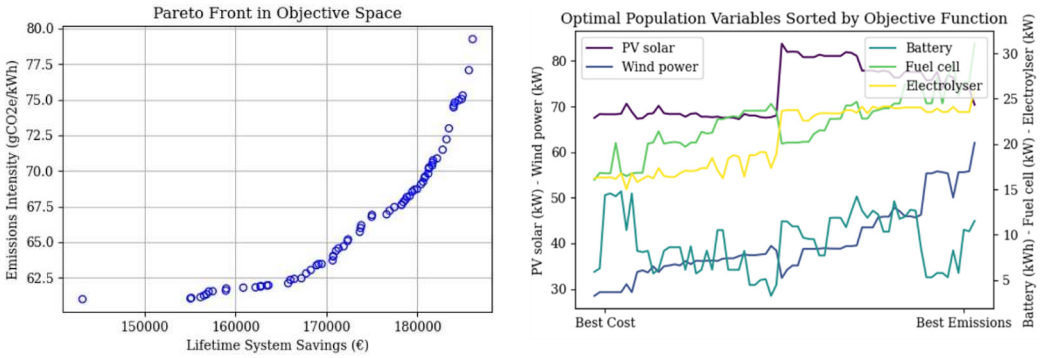


(**a**) Pareto front in objective space. (**b**) Optimal variables sorted by objective.

**Figure 9.** key outputs from the multi-objective optimisation process, indicating relationship between cost reduction and climate impact of the system design.

The graph in Figure 9b displays the capacities of PV solar, wind power, battery, fuel cell, and electrolyser systems with the final population arranged by the two objective functions. The best economic outcome is on the left, while the best environmental outcome is on the right. It is observed that all systems generally tend towards an increase in capacity as the emissions improve. This is most likely because a larger total off-grid capacity has a higher self-consumption rate, and therefore is relying less on the grid which has a high emissions intensity of 325 gCO2e/kWh. The REC is consequently able to reduce emissions to a greater extent. This, of course, negatively impacts the economics of the REC as more capital has to be invested into a more substantial design. It appears from the graph that the wind power, as well as the fuel cell and electrolyser which make up the RHFC are most sensitive to changes in the objective functions. The following section explores the chosen optimal design, and details why the capacities affect the objective functions in this way.

### *4.2. Best hybrid system design for the Renewable Energy Community*

The pareto front provides a range of potential non-dominated solutions in which neither objective function is favoured over the other. The are several methods that can be used the choose a nominally 'best' system from the population to perform further analysis. Based on the research conducted by Wang and Rangaiah [66], it was chosen to use Simple Additive Weighting (SAW). SAW normalises both objective function values, where zero is the worst possible result and one is the most improved. The values are then summed for each member of the population to find the best overall solution. Weighting can be applied to the objective functions, but for this case neither is favoured over the other.

$$\begin{cases} F_{ij} = \dfrac{f_{ij}}{f_j^+} \text{ for a maximisation criterion, where } f_i^+ = \mathrm{Max}_{i\in m} f_{ij} \\ F_{ij} = \dfrac{f_{ij}}{f_j^-} \text{ for a minimisation criterion, where } f_i^- = \mathrm{Min}_{i\in m} f_{ij} \end{cases} \tag{16}$$

$$A_i = \sum_{j=1}^{n} F_{ij} \tag{17}$$

$F_{ij}$ is the normalised set of objective functions $j$ for pareto population $i$, $f_{ij}$ is the initial set, and $f_{j+}$ is and $f_{j-}$ is the maximum and minimum criteria of the set, respectively. $A_i$ then provides the best set of design variables to use in the hybrid REC, given in Table 5. The system was then simulated to perform analysis of all performance indicators.

Preprints (www.preprints.org) | NOT PEER-REVIEWED | Posted: 7 August 2023 doi:10.20944/preprints202308.0471.v1



**Table 5.** Optimal installed capacities of the energy system assets.

| REC Asset | Optimal Values |
|---|---|
| PV Solar | 71 kW |
| Wind Turbine(s) | 32 kW |
| Lithium Battery | 14 kWh |
| PEM fuel cell | 20 kW |
| AEM ELectrolyser | 18 kW |

Figure 10 contains two one-week sample periods obtained from the simulation, displaying the balance of each asset and their contribution to balancing the total REC load. Typical summer and winter periods are used to observe the seasonal variation in system response. The REC load is higher on average during the summer period, leading to increased reliance and the energy grid to fill gaps in the consumption requirement when the ESS is unavailable. The winter period, by contrast, is able to satisfy the load requirement with the exception of some short periods. This shows that although the REC can operate largely off-grid, it is still beneficial from both an economic and emissions perspective to remain grid-connected from the short period when the REC generation and hybrid storage cannot fully balance the consumption. The hydrogen system requires a maximum storage of 1835k, which is evaluated from the simulation as the storage required to avoid any state-of-charge limits. The value therefore is a worst-case scenario for the system, as it is likely that a smaller storage would be chosen in accordance with the installation space available within the REC. Given the Lower Heating Value (LHV) of hydrogen and the average fuel cell efficiency of 46%, the system would require approximately 14 $Nm^2$ of hydrogen stored at 35bar to supply the required quantity of a one-year period.

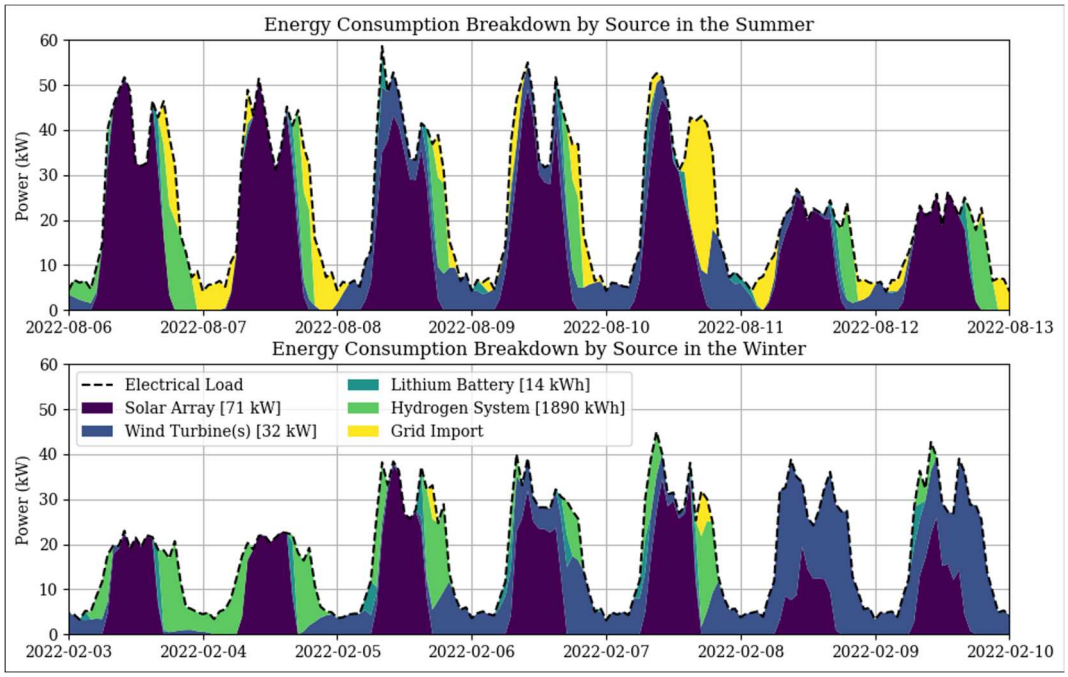


**Figure 10.** Energy generation hour-by-hour breakdown by source. Example shown includes typical summer and winter weeks.

Table 6 below shows a full breakdown of the economic and environmental performance of each grouped asset. The solar array is able to deliver the most energy to the REC due to the high capacity of 71 kW, but also the higher solar potential on the island of Formentera of 4.7 kWh/m2, compared to London, UK, of 2.9 kWh/m2. Energy generated from wind provides the next greatest portion of over

Preprints (www.preprints.org) | NOT PEER-REVIEWED | Posted: 7 August 2023 doi:10.20944/preprints202308.0471.v1



24%, the benefit of which is that energy is generated during the night period as well as the day to charge the battery and a steady quantity of hydrogen. The battery itself is relatively small compared to the other components at 14 kWh and responds only when energy generated is no longer available in excess of supply. The fuel cell and electrolyser were sized at 20 kW and 18 kW, respectively. It is interested to note that the electrolyser is smaller in power input capacity than the fuel cell, even though the efficiencies would dictate the fuel cell would need to approximately half the rated power of the electrolyser to achieve the same capacity factor. The increased generation from wind power over a more of the simulation may allow the electrolyser to run for longer periods and make up the fuel cell's lower efficiency.

4.2.1. Techno-economic Assessment

It is important to analyse each component on an individual basis to understand fully their contribution to the economic and emissions performance within the system. This not only would help confirm the results seen in the pareto optimality, but also from a practical perspective assist a potential system designer to identify the most important assets, any particularly sensitive parameters, and assess the risks associated with each.

**Table 6.** The economic and environmental performance of the different REC assets in the optimal design configuration.

| Technology Asset | Energy-Delivered (kWh) | Capacity-Factor (%) | CAPEX (€) | OPEX (€/year) | LCOE (€/kWh) | Emissions (gCO2e/kWh |
|---|---|---|---|---|---|---|
| PV Solar [71 kW] | 141184 | 19 | 177500 | 2130 | 0.07 | 40.7 |
| Wind Turbine(s) [32 kW] | 60517 | 22 | 91200 | 1024 | 0.09 | 15.9 |
| Lithium Battery [14 kWh] | 4910 | 8 | 5446 | 308 | 0.08 | 72.4 |
| Hydrogen System [1836 kWh] | 26360 | 15 | 106000 | 570 | 0.17 | 18.6 |

The solar array has the largest capital and operational costs compared with the wind power alternative due to the higher unit costs per kW. Despite this, since the PV solar is able to achieve a greater capacity factor, which is the measure of energy output as a ratio of the total potential output of the same period. PV solar is naturally limited by the hours of solar available, while wind power is limited by the average wind speed and distribution. The higher capacity is the main mechanism which produces a lower LCOE for the PV solar of 0.07 compared with wind power's 0.09 €/kWh, despite the higher CAPEX and OPEX costs. This result also implies that although wind power is possible on with the REC, it may be beneficial from a to study a PV solar generation only option due to the potential impracticalities of local wind turbines. The inverse is then observed for the environmental impact, in that the PV solar has considerably higher embedded emissions of 40.7 gCO2e/kWh compared with 15.9 gCO2e/kWh expected from equivalent wind energy. This confirms

Preprints (www.preprints.org) | NOT PEER-REVIEWED | Posted: 7 August 2023 doi:10.20944/preprints202308.0471.v1



the previous observation in Figure 11, where the wind capacity is small at the best net savings but grows as the net emissions improve. The hybrid ESS is somewhat unbalanced as the optimisation favours a relatively small battery compared with large capacity for hydrogen. This is due in part to the different roles the two assets assume, in that the battery is used daily for quick response, whereas the hydrogen system is much better suited to long term seasonal storage which requires far more capacity.

At 106k€, the RHFC CAPEX is a factor of twenty higher than the battery. This trend carries over into the LCOE results, where an approximate doubling of the levelized cost is observed for the hydrogen system compared with lithium batteries. It is widely known that hydrogen technology is a less financially viable alternative for many applications, so this result was somewhat expected. This could change in the near future as costs of hydrogen technology reduce. T he interest comes, however, when analysing the emissions intensity. The emissions output from the battery per kWh delivery is far higher than the hydrogen solution at 72.4 and 18.6 gCO2e/kWh, respectively. The trend is also supported by the population variables in Figure 9b, in which its noted that as the hydrogen assets increase in capacity, the emissions result improves, while the net savings deteriorate.

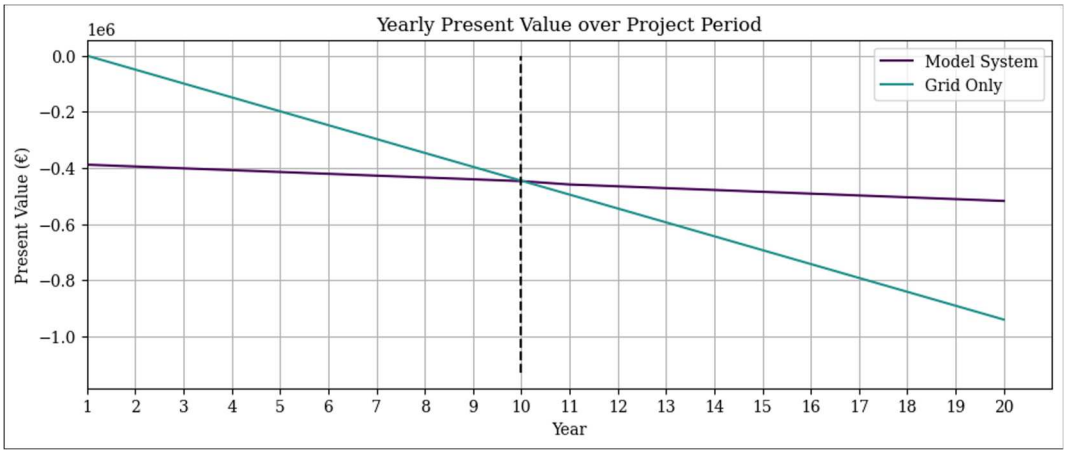


**Figure 11.** The Present Value over project period. The system is primarily compared with a 'businessas-usage' grid only scenario.

A direct comparison to the 'business-as-usual' grid-only case is used to observed the improvements in the economics with a decentralised REC architecture. Figure 11 contains the present value curve of the grid-only case, that is when electricity cost is paid to the utility company over the project period. The curve starts at zero as there is no capital cost associated with grid usage, but the operational cost per year is high. By contrast, the modelled REC requires an initial investment of 380k€. However, the lower year-on-year cost means that the system can pay off the investment cost, described as the payback term, in 9 years. The project ends with a final total savings of 178k€when the inflation and discounts rates of 2% and 5%, respectively, are considered. The result produces an IRR of 10.9%, years returns of 9.6%, and an average system LCOE of 0.16 €/kWh. This assessment is based on the cost of equipment and installation since 2020.

Considering the historical and currently observed trends in renewable generation and storage equipment cost, it is projected that by 2030 and beyond there will continue to be a substantial decrease in the financial requirements for this type of system. The results shown here are therefore towards the upper bounds in terms of uncertainty about the future cost of an REC implementation.

### 4.2.2. REC members' net savings and environmental impacts

The model not only provides a global view of the potential impact of an REC configuration but is also able to analyse the reduce in cost and emissions on a per load basis. There are seven discretised loads within the model, with each being able to mutually accept and trade energy with the decentralised assets. Table 7 below shows the average LCOE and emissions intensity for each building and the percentage decrease in emissions. The REC can provide a considerable degree of

Preprints (www.preprints.org) | NOT PEER-REVIEWED | Posted: 7 August 2023 doi:10.20944/preprints202308.0471.v1



self-consumption, ranging from 91.1% for the largest load to over 98% for the smallest. In terms of impact on the energy cost, the new LCOE ranges 0.16-0.17 €/kWh compared to 0.30 €/kWh for grid-only. The decarbonisation of energy usage was also seen to be in the range 75-77% in the first year of installation.

**Table 7.** The economic and environmental performance of the different REC assets in the optimal design configuration.

| REC member | REC delivered (kWh) | Grid delivered (kWh) |
|---|---|---|
| Community Centre | 61078 | 5461 |
| Elementary school | 18807 | 348 |
| High school | 44743 | 1437 |
| Council offices | 28244 | 683 |
| Residential units | 11975 | 514 |

*4.3. Best case and extremes comparison*

It is vital to understand not only the characteristics of the system at the 'best' pareto result, but also the performance at the extremes of the multi-objective optimisation. The result gives an indication as to how sensitive the result is to changing parameters. Table 8 contains the results of the three chosen REC configurations in terms of hybrid generation and storage capacities.

**Table 8.** Comparison REC configurations for extreme cases for net savings and decarbonisation potential compared with the chosen nominal case.

| | Best net savings | Nominal | Best emissions savings |
|---|---|---|---|
| REC Delivered (kWh) | 151493 | 156536 | 158823 |
| Self-Consumption (%) | 91.0 | 94.5 | 96.2 |
| LCOE (€/kWh) | 0.15 | 0.16 | 0.19 |
| Net Savings (€) | 187080 | 178229 | 139647 |
| Savings (%) | 51 | 47 | 36 |
| IRR (%) | 12.6 | 10.9 | 7.1 |
| Simple Payback (%) | 10.1 | 9.6 | 8.0 |
| Payback Term (years) | 8.3 | 9.0 | 11.5 |
| Emissions (gCO2e/kwh) | 79 | 69 | 61 |
| Decarbonisation (%) | 75.6 | 78.8 | 81.2 |

*4.4. Pareto front comparison of energy storage system technologies*

The hybrid ESS comprised of a lithium battery and RHFC system produces differing performance outcomes based on the relative capacities of the technologies. Therefore, a comparison of the multi-objective optimisation for the same REC set-up with an additional battery only ESS and RHFC only ESS are required to ensure that the hybrid design is able to provide the best performance in terms of environmental impact and cost savings for the REC members. Figure 12 compares these pareto fronts, from which the combination of the technologies is able to provide a significant

Preprints (www.preprints.org) | NOT PEER-REVIEWED | Posted: 7 August 2023 doi:10.20944/preprints202308.0471.v1



improvement over the technologies working independently. This is likely due to the fact that the battery is better at providing a short-term response but suffers from increased degradation if used frequently for charge and discharge, and similarly the hydrogen system requires high capital cost and is best suited to long term storage of grid energy. The battery alone also more embedded carbon, which limits its ability to decarbonise. The hydrogen only suffers from the limitation that the electrolyser only runs at rated power, limited flexibility.

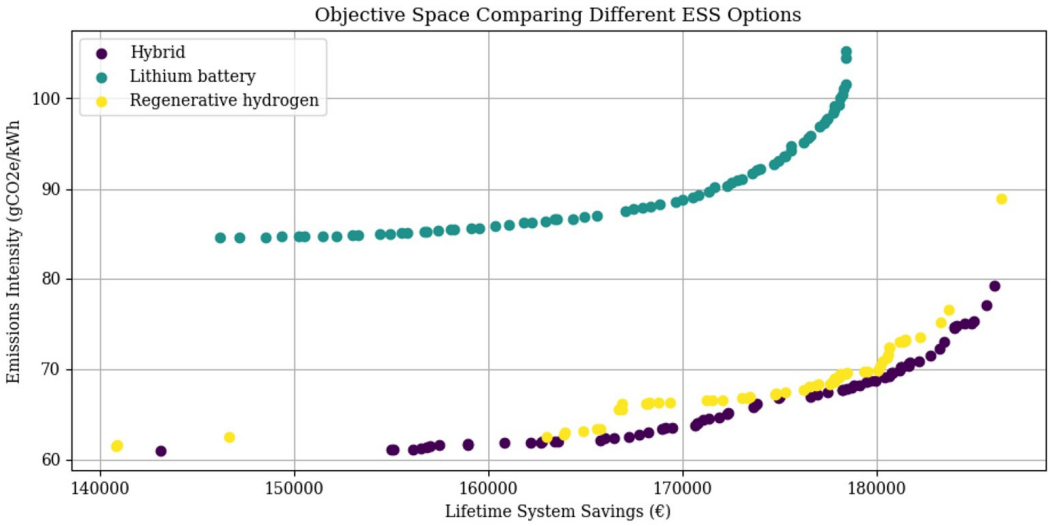


**Figure 12.** The Present Value over project period. The system is primarily compared with a 'businessas-usage' grid only scenario.

In combination, the battery is likely able to smooth out some of these variations and provide the best overall solution.

## 5. Conclusions

This work presents a novel decentralised hybrid generation and ESS implementing both battery and hydrogen technology for use in geographically isolated rural Renewable Energy Community. A review of existing state-of-the-art was presented and highlighted the gaps in knowledge for such a system, particularly when considering both economic feasibility and a dynamic calculation of the environmental impact. This discussion comes at an interesting time for Europe and around the world as policymakers work to facilitate the potential benefits of aggregating decentralised renewables, one such method being the REC. The steady cost reduction in PV solar and wind power as seen over the past years has also accelerated growth in the decentralised energy sector. The rise of cost-effective hydrogen technology is set to make considerable impact on how energy is stored and transported as a vector.

The results from this study show that there is an inherent trade-off relationship between cost reduction and ability to decarbonise the energy system. By using a model built in Python, several different economic and environmental scenarios can be assessed. The implementation of a multi-objective algorithm gives potential system designers and policymakers a range of possible solutions. In this case, the optimal design results in an LCOE of 0.15€/kWh, a project IRR of 10.8% and ROI of 9 years. Greenhouse gas emissions is reduced by 72% in the first year of installation to 69 gCO2e/kWh. In further studies, emphasis should be placed on performing a sensitivity analysis and understanding where uncertainty may arise in the energy model, which would give a better understanding of which input parameters risk changing the outcome of the model. Additionally, research into the implementation of REC architectures in other countries around the world would also give a global perspective of how effective an REC could be in keeping energy cost stable and curbing the impacts of climate change.

**Funding:** This research is sponsored by the EU Horizon 2020 research and innovation program under grant agreement No 957852: Virtual Power Plant for Interoperable and Smart isLANDS-VPP4ISLANDS. More information available at https://cordis.europa.eu/project/id/957852.

**Acknowledgments:** Special thank you to the Consel de Formentera for allowing access to energy consumption data, from which the energy community model was built.

**Conflicts of Interest:** The authors declare no conflict of interest.

### Abbreviations

The following abbreviations are used in this manuscript:

| | |
|---|---|
| CAPEX | Capital Expenditure |
| DOD | Depth of Discharge |
| ESS | Energy Storage System |
| GA | Genetic Algorithm |
| GHI | Global Horizontal Irradiance |
| GWP | Global Warming Potential |
| IEC | International Electrotechnical Commission |
| IRR | Internal Rate of Return |
| LCOE | Levelised Cost of Electricity |
| NPV | Net Present Value |
| NSGA | Non-dominated Sorting Genetic Algorithm |
| OPEX | Operational Expenditure |
| PEM | Proton Exchange Membrane |
| PV | Photovoltaic |
| REC | Renewable Energy Community |
| RED | Renewable Energy Directive |
| RES | Renewable Energy System |
| RHFC | Regenerative Hydrogen Fuel Cell |
| ROI | Return on Investment |
| SOC | State of Charge |
| TSO | Transmissions System Operator |

## References

1. United Nations. *The Paris Agreement*; United Nations: Paris, France, sn, 2015.
2. Intergovernmental Panel on Climate Change. *Synthesis Report of the IPCC Sixth Assessment Report (AR6*; IPCC Secretariat: Geneva, Switzerland, 2022.
3. Wang, R. Achieving ecological sustainability through technological innovations, financial development, foreign direct investment, and energy consumption in developing European countries. *Gondwana Research* **2023**, *119*, 138–152.
4. Department for Business, E.; Strategy, I. *British Energy Security Strategy*; HM Goverment UK: London, UK, 2022.
5. Boie, I.; Fernandes, C.; Frias, P.; Klobasa, M. Efficient strategies for the integration of renewable energy into future energy infrastructures in Europe – An analysis based on transnational modeling and case studies for nine European regions. *Energy Policy* **2014**, *67*, 170–185.
6. Kabeyi, M.; Olanrewaju, O. Sustainable Energy Transition for Renewable and Low Carbon Grid Electricity Generation and Supply. *Front Energy Res* **2022**, *9*, 743114.
7. Gielen, D. The role of renewable energy in the global energy transformation. *Energy Strategy Reviews* **2019**, *24*, 38–50.

8. Saboori, H.; Mohammadi, M.; Taghe, R. Virtual Power Plant (VPP), Definition, Concept, Components and Types. In Proceedings of the 2011 Asia-Pacific Power and Energy Engineering Conference, 2011.
9. Hirth, L.; Ziegenhagen, I. Balancing power and variable renewables: Three links. *Renewable and Sustainable Energy Reviews* **2015**, *50*, 1035–1051.
10. Mohd Azmi, K. Active Electric Distribution Network: Applications, Challenges, and Opportunities. *IEEE Access* **2022**, *10*, 134655–134689.
11. Rezaeimozafar, M.; Monaghan, R.; Barrett, E.; Duffy, M. A review of behind-the-meter energy storage systems in smart grids. *Renewable and Sustainable Energy Reviews* **2022**, *164*, 112573.
12. Aneke, M.; Wang, M. Energy storage technologies and real life applications – A state of the art review. *Applied Energy* **2016**, *179*, 350–377.
13. Hesse, H.; Schimpe, M.; Kucevic, D.; Jossen, A. Lithium-Ion Battery Storage for the Grid—A Review of Stationary Battery Storage System Design Tailored for Applications in Modern Power Grids. *Energies* **2017**, *10*, 2107.
14. Wali, S. Grid-connected lithium-ion battery energy storage system: A bibliometric analysis for emerging future directions. *Journal of Cleaner Production* **2022**, *334*, 130272.
15. Vykhodtsev, A. A review of modelling approaches to characterize lithium-ion battery energy storage systems in techno-economic analyses of power systems. *Renewable and Sustainable Energy Reviews* **2022**, *166*, 112584.
16. Zhang, W.; Maleki, A.; Rosen, M.; Liu, J. Optimization with a simulated annealing algorithm of a hybrid system for renewable energy including battery and hydrogen storage. *Energy* **2018**, *163*, 191–207.
17. French, S. The Role of Zero and Low Carbon Hydrogen in Enabling the Energy Transition and the Path to Net Zero Greenhouse Gas Emissions : With global policies and demonstration projects hydrogen can play a role in a net zero future. *Johnson Matthey Technology Review* **2020**, *64*, 357–370.
18. Coppitters, D.; Paepe, W.; Contino, F. Robust design optimization and stochastic performance analysis of a grid-connected photovoltaic system with battery storage and hydrogen storage. *Energy* **2020**, *213*, 118798.
19. Haji Bashi, M. A review and mapping exercise of energy community regulatory challenges in European member states based on a survey of collective energy actors. *Renewable and Sustainable Energy Reviews* **2023**, *172*, 113055.
20. European Parliament. *Directive (EU) 2018/2001 of the European Parliament and of the Council of 11 December 2018 on the promotion of the use of energy from renewable sources*; European Parliament: Brussels, Belgium, 2018.
21. Fina, B.; Monsberger, C. Legislation for renewable energy communities and citizen energy communities in Austria: changes from the legislative draft to the finally enacted law. *Journal of World Energy Law Business* **2022**, *15*, 237–244.
22. Sebi, C.; Vernay, A.L. Community renewable energy in France: The state of development and the way forward. *Energy Policy* **2020**, *147*, 111874.
23. Broska, L.; Vögele, S.; Shamon, H.; Wittenberg, I. On the Future(s) of Energy Communities in the German Energy Transition: A Derivation of Transformation Pathways. *Sustainability* **2022**, *14*, 3169.
24. Swens, J.; Diestelmeier, L. Developing a legal framework for energy communities beyond energy law. *Energy Communities sl:Academic Press* **2022**, p. 59–71.
25. Trevisan, R.; Ghiani, E.; Pilo, F. Renewable Energy Communities in Positive Energy Districts: A Governance and Realisation Framework in Compliance with the Italian Regulation. *Smart Cities* **2023**, *6*, 563–585.
26. Gallego-Castillo, C.; Heleno, M.; Victoria, M. Self-consumption for energy communities in Spain: A regional analysis under the new legal framework. *Energy Policy* **2021**, *150*, 112144.
27. Official Gazette. Legislative Decree no. *Official Gazette* **2021**.
28. Di Silvestre, M. Energy self-consumers and renewable energy communities in Italy: New actors of the electric power systems. *Renewable and Sustainable Energy Reviews* **2021**, *151*, 111565.
29. Trevisan, R. Optimal Sizing of a PV and Storage for a Port Renewable Energy Community, 2022.
30. Bartolini, A.; Carducci, F.; Munoz, C. Energy storage and multi energy systems in local energy communities with high renewable energy penetration. *Renewable Energy* **2020**, *159*, 595–609.
31. Wang, W. Techno-economic analysis of the transition toward the energy self-sufficiency community based on virtual power plant. *Front Energy Res* **2023**, *11*.

32. Cuesta, M.; Castillo-Calzadilla, T.; Borges, C. A critical analysis on hybrid renewable energy modeling tools: An emerging opportunity to include social indicators to optimise systems in small communities. *Renewable and Sustainable Energy Reviews* **2020**, *122*, 109691.
33. Niveditha, N.; Rajan Singaravel, M. Optimal sizing of hybrid PV–Wind–Battery storage system for Net Zero Energy Buildings to reduce grid burden. *Applied Energy* **2022**, *324*, 119713.
34. Zhang, Y. Capacity configuration optimization of multi-energy system integrating wind turbine/photovoltaic/hydrogen/battery. *Energy* **2022**, *252*, 124046.
35. Xu, C. Data-driven configuration optimization of an off-grid wind/PV/hydrogen system based on modified NSGA-II and CRITIC-TOPSIS. *Energy Conversion and Management* **2020**, *215*, 112892.
36. Xuan, J. Optimal planning of hybrid electric-hydrogen energy storage systems via multi-objective particle swarm optimization. *Front Energy Res* **2022**, *10*, 1034985.
37. He, Y. Multi-objective planning-operation co-optimization of renewable energy system with hybrid energy storages. *Renewable Energy* **2022**, *184*, 776–790.
38. Wang, H. Energy management strategy of hybrid energy storage based on Pareto optimality. *Applied Energy* **2022**, *327*, 120095.
39. NASA. LARC Power Data Access Viewer, 2023.
40. Farhad, A.; Ali, G.; Mohsen, J. *Dataset on Hourly Load Profiles for a Set of 24 Facilities from Industrial, Commercial, and Residential End-use Sectors*; Mendeley Data, 2020; p. 1.
41. Pinto, E.; Serra, L.; Lázaro, A. Energy communities approach applied to optimize polygeneration systems in residential buildings: Case study in Zaragoza, Spain. *Sustainable Cities and Society* **2022**, *82*, 103885.
42. Chung, M. Economic Evaluation of Renewable Energy Systems for the Optimal Planning and Design in Korea – A Case Study. *Journal of Sustainable Development of Energy, Water and Environment Systems* **2018**, *6*, 725–741.
43. Duffie, J.; Beckman, W. *Solar Engineering of Thermal Processes*; Wiley: Hoboken, 1991.
44. Reda, I.; Andreas, A. *Solar Position Algorithm for Solar Radiation Applications*; National Renewable Energy Laboratory: Golden, Colorado, 2008.
45. Corke, T.; Nelson, R. *Wind Energy Design*; Taylor Francis Group: Miami Florida, 2018.
46. Wood, D. *Improvements to the Simplified Loads Methodology in IEC 61400-2*; National Renewable Energy Laboratory: Golden, CO, 2021.
47. Draxl, C.; Clifton, A.; Hodge, B.M.; McCaa, J. The Wind Integration National Dataset (WIND) Toolkit. *Applied Energy* **2015**, *151*, 355–366.
48. Shepard, C. Design of Primary and Secondary Cells: II An Equation Describing Battery Discharge. *Journal of The Electrochemical Society* **1965**, *112*.
49. Burton, T.; Sharp, D.; Jenkins, N.; Bossanyi, E. *Wind Energy Handbook*; John Wiley Sons: West Sussex, 2001.
50. Warner, S.; Hussain, S. *The Finance Book*; Pearson Education Ltd: Harlow, 2017.
51. Jansen, G.; Dehouche, Z.; Corrigan, H. Cost-effective sizing of a hybrid Regenerative Hydrogen Fuel Cell energy storage system for remote off-grid telecom towers. *International Journal of Hydrogen Energy* **2021**, *46*.
52. Feldman, D.; Dummit, K.; Zuboy, J.; Margolis, R. *Fall 2022 Solar Industry Upyear*; National Renewable Energy Laboratory: Golden, Colorado, 2022.
53. Carvalho, M.; Menezes, V.; Gomes, K.; Pinheiroc, R. Carbon Footprint Associated with a Mono-Si Cell Photovoltaic Ceramic Roof Tile System. *Sustainable Energy* **2019**, *38*.
54. Stehly, T.; Beiter, P.; Duffy, P. *2019 Cost of Wind Energy Review*; National Renewable Energy Laboratory: Golden, Colorado, 2019.
55. Intergovernmental Panel on Climate Change. *Climate Change 2021: The Physical Science Basis Contribution of Working Group I to the Sixth Assessment Report of the Intergovernmental Panel on Climate Change*; Cambridge University Press: Cambridge, UK, 2021.
56. Mongird, K. *2020 Grid Energy Storage 2020 Grid Energy Storage Performance Assessment*; US Department of Energy: Richland, Washington, 2020.
57. Romare, M.; Dahllöf, L. *The Life Cycle Energy Consumption and Greenhouse Gas Emissions from Lithium-Ion Batteries*; IVL Swedish Environmental Research Institute: Stockholm, Sweden, 2017.
58. Ballard. *Fuel Cell Life cycle Assessment, Burnaby*; Ballard: Burnaby, Canada, 2018.
59. Department for Business, E.; Strategy, I. *Hydrogen Production Costs*; HM Government UK: London, UK, 2021.
60. Enapter. A small carbon footprint for big climate impact, 2022.

61. Reddi, K.; Elgowainy, A.; Rustagi, N.; Gupta, E. Techno-economic analysis of conventional and advanced high-pressure tube trailer configurations for compressed hydrogen gas transportation and refueling. *International Journal of Hydrogen Energy* **2018**, *43*, 4428–4438.
62. Agostini, A. Role of hydrogen tanks in the life cycle assessment of fuel cell-based auxiliary power units. *Applied Energy* **2018**, *215*, 1–12.
63. *Comparative life cycle assessment for PEMFC stack including fuel storage materials in UAE*, 2020.
64. Deb, K.; Pratap, A.; Agarwal, S.; Meyarivan, T. A Fast and Elitist Multiobjective Genetic Algorithm: NSGA-II. *Transactions on Evolutionary Computation* **2002**, *6*, 182–197.
65. Blank, J.; Deb, K. pymoo: Multi-Objective Optimization in Python. *IEEE Access* **2020**, *8*, 89497–89509.
66. Wang, Z.; Rangaiah, G. Application and Analysis of Methods for Selecting an Optimal Solution from the Pareto-Optimal Front obtained by Multiobjective Optimization. *Industrial Engineering Chemistry Research* **2017**, *56*, 560–574.